Acta Cryst E CRYSTALLOGRAPHIC COMMUNICATIONS
ISSN 2056-9890

A mixed phosphine sulfide/selenide structure as an instructional example for how to evaluate the quality of a model

Sean Parkin,[a]* Jeremy Cunningham,[b] Brian Rawls,[b] John E. Bender,[b] Richard J. Staples[c] and Shannon M. Biros[b]*

[a]Department of Chemistry, University of Kentucky, Lexington, KY, 40506, USA, [b]Department of Chemistry, Grand Valley State University, Allendale, MI 49401, USA, and [c]Center for Crystallographic Research, Department of Chemistry, Michigan State University, East Lansing, MI 48824, USA. *Correspondence e-mail: s.parkin@uky.edu, biross@gvsu.edu

Received 27 February 2023
Accepted 22 March 2023

Edited by G. Diaz de Delgado, Universidad de Los Andes Mérida, Venezuela

Keywords: checkCIF alerts; F^2_{obs} *vs* F^2_{calc}; OMIT command; outliers; displacement ellipsoids; solid solution; disordered electron density; standard interatomic distances; crystal structure.

CCDC reference: 2231833

Supporting information: this article has supporting information at journals.iucr.org/e

This paper compares variations on a structure model derived from an X-ray diffraction data set from a solid solution of chalcogenide derivatives of *cis*-1,2-bis(diphenylphosphanyl)ethylene, namely, 1,2-(ethene-1,2-diyl)bis(diphenylphoshpine sulfide/selenide), $C_{26}H_{22}P_2S_{1.13}Se_{0.87}$. A sequence of processes are presented to ascertain the composition of the crystal, along with strategies for which aspects of the model to inspect to ensure a chemically and crystallographically realistic structure. Criteria include mis-matches between F^2_{obs} and F^2_{calc}, plots of $|F_{obs}|$ *vs* $|F_{calc}|$, residual electron density, *checkCIF* alerts, pitfalls of the OMIT command used to suppress ill-fitting data, comparative size of displacement ellipsoids, and critical inspection of interatomic distances. Since the structure is quite small, solves easily, and presents a number of readily expressible refinement concepts, we feel that it would make a straightforward and concise instructional piece for students learning how to determine if their model provides the best fit for the data and show students how to critically assess their structures.

1. Chemical context

Our research group has synthesized a number of phosphine chalogenide derivatives and explored their chemistry in regard to their coordination with both *d*-block and *f*-block metals (Luster *et al.*, 2022; Mugemana *et al.*, 2018; Morse *et al.*, 2016; Neils *et al.*, 2022). A few years ago, we worked with the rigid diphosphine *cis*-1,2-bis(diphenylphosphine)ethylene **1** (*cis*-dppe), and developed conditions for the synthesis of the di-sulfide **2** (Rawls *et al.*, 2023) and the di-selenide **3** (Jones *et al.*, 2015) (Fig. 1). We obtained X-ray diffraction data for both **2** and **3**, and the structures were isomorphic, having the symmetry of the orthorhombic space group $P2_12_12_1$. Our synthetic efforts then turned to preparation of mono-selenide **4** as a way to gain access to the mixed sulfide-selenide system, **5**.

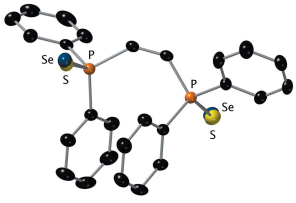

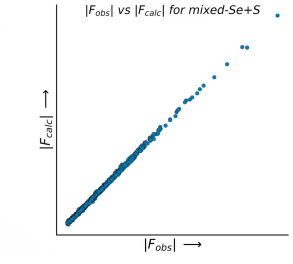

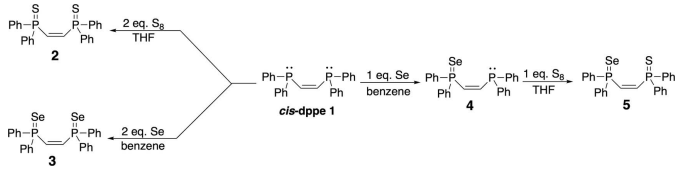

Figure 1
A generalized reaction scheme to prepare the compounds studied in this work.

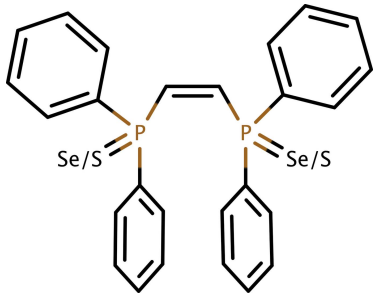

2. Structure solution and model building trials

We obtained diffraction data for crystals grown directly from the reaction mixture. The structure solved easily in $P2_12_12_1$ using *SHELXT* (Sheldrick, 2015*a*) with included scattering factors for C, H, P, Se and a unit cell that was clearly related to those of compounds **2** and **3**. In the initial solution, however, *SHELXT* had assigned scattering factors for phosphorus to both chalcogen sites, a chemical impossibility. In terms of similarity of scattering factors, sulfur would be the obvious next choice for the chalcogen, but the pnictogen-to-chalcogen distances (*vide infra*) were much longer than in the di-sulfide structure **2** (Rawls *et al.*, 2023). Given the available electron density at the chalcogen site, a disordered mono-selenide model seemed plausible. Of paramount importance here is that any trial model must be chemically plausible, thus knowledge of chemistry and information from other spectroscopic techniques (if available) should be used to rule out alternatives.

2.1. Trial 1: a mono-selenide model

Manual editing of the chalcogen sites to accommodate a single Se atom split over the two sites gave a model that refined smoothly using *SHELXL* (Sheldrick, 2015*b*), giving a disordered Se occupancy ratio of 0.526 (2):0.474 (2) (Fig. 2*a*). The P═Se distances were 2.063 (2) and 2.035 (2) Å, and the model converged to an R_1 value of 0.0494.

This model passed all the typical *checkCIF* tests, apart from returning a *B*-level alert indicating the presence of a few reflections with a poor fit between F^2_{obs} and F^2_{calc} The *SHELXL* list of 'most disagreeable reflections' (*i.e*, mis-matches between observed and calculated data) showed a striking difference for four reflections (Table 1, Fig. 2*b*). At this point, it might be tempting to simply remove the top few poorly fitting reflections (*i.e.*, those having error/s.u. > 10) using the OMIT command in *SHELXL* and be satisfied with the structure. However, *all* of the worst outliers (see Table 1) have $F^2_{obs} >> F^2_{calc}$ and are at resolutions far removed from the beamstop shadow. Thus, the commonly blamed culprit of 'obscured by the beamstop' would not provide any justification for omission. Unfortunately, uncritical omission of the worst-offending reflections in order to suppress unfavourable *checkCIF* alerts has become all too common. When $F^2_{obs} >> F^2_{calc}$, however, such ill-fitting intensities are precisely the datapoints that are most sensitive to any model deficiencies. Modern data-reduction software includes facilities to identify the particular frame for any such outliers for manual inspection. In the present case, the offending reflections appeared to have been measured properly; no justification for omission

Table 1
List of the top four poorly fitting reflections for the model of the mono-selenide shown in Fig. 2.

h k l	F^2_{obs}	F^2_{calc}	*error/s.u.*	$F_{calc}/F_{calc(max)}$	*d–spacing* (Å)
1 0 2	250.91	6.81	10.42	0.012	6.16
0 3 2	1787.72	504.88	10.20	0.101	3.74
2 0 3	335.44	41.35	9.52	0.029	3.76
1 4 0	671.93	175.18	8.75	0.060	3.18

All of the worst fitting reflections above have $F^2_{obs} >> F^2_{calc}$ and *none* would be obscured by a well-designed beamstop.

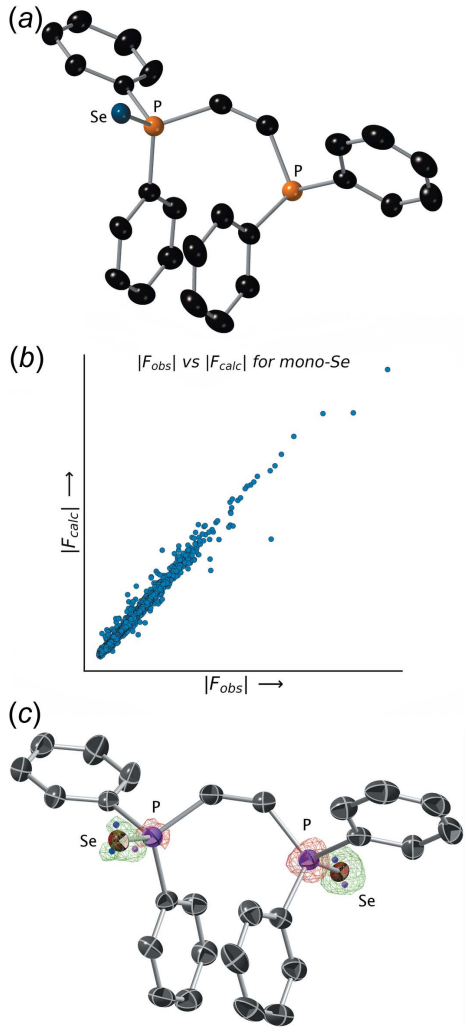

Figure 2
(*a*) An ellipsoid (50% probability) plot for the major component of the mono-selenide model. (*b*) A plot of $|F_{obs}|$ *vs* $|F_{calc}|$ values for the mono-selenide model. Note the extent of scatter in the plot. (*c*) A difference-electron density map reveals positive (green) electron density at the chalcogen site and negative (red) contours at the phosphorus sites. Small peaks within the positive density are represented by coloured dots. The single Se atom in trial 1 is split with occupancies of 0.526 (2) and 0.474 (2) over the two chalcogen sites.

was apparent. A closer look at the model showed that the displacement ellipsoids for the Se atoms were a little on the small side relative to neighbouring atoms, and that the residual difference-Fourier map showed pronounced electron density with several small embedded difference-map peaks (each less than 0.9 e Å^{-3}) clustered near the chalcogen sites (Fig. 2*c*). These 'features' suggest that this model did not fully account for all the electron density present in the data.

2.2. Trial 2: a di-selenide model

To better account for the residual electron density, we built a model that corresponded to the di-selenide **3**, in which each Se atom had a fixed occupancy of 1.0 (Table 2 and Fig. 3). The resulting P═Se distances were (unsurprisingly) similar to those for the previous model at 2.061 (2) and 2.030 (2) Å. However, the R_1 value for this model jumped to 0.0632 and the mis-match between the values of the displacement parameter tensors for the Se atoms and those for the rest of the atoms in the structure became wholly unrealistic (Fig. 3*a*). Moreover, the discrepancy between the top four 'disagreeable' reflections became even larger, and the $|F_{obs}|$ *vs* $|F_{calc}|$ plot was a little more scattered (Fig. 3*b*). By any measure, the di-selenide model is demonstrably worse than the mono-selenide model. Comparison of these two models, however, suggests that the electron density for the chalcogen atom sites present in the crystal that produced the diffraction data was insufficient to support two fully occupied selenium atoms, but it was too much for a mono-selenide model.

Table 2
List of the top four poorly fitting reflections for the model of the di-selenide shown in Fig. 3.

h k l	F^2_{obs}	F^2_{calc}	*error/s.u.*	$F_{calc}/F_{calc(max)}$	*d–spacing* (Å)
1 2 0	14663.16	2109.28	11.62	0.181	5.80
4 2 0	1787.72	13.29	10.10	0.014	2.78
0 4 3	335.44	114.61	10.00	0.042	2.71
0 2 0	671.93	1634.82	9.55	0.159	6.58

Three of the worst fitting reflections above have F^2_{obs} >> F^2_{calc} and *none* would be obscured by a well-designed beamstop.

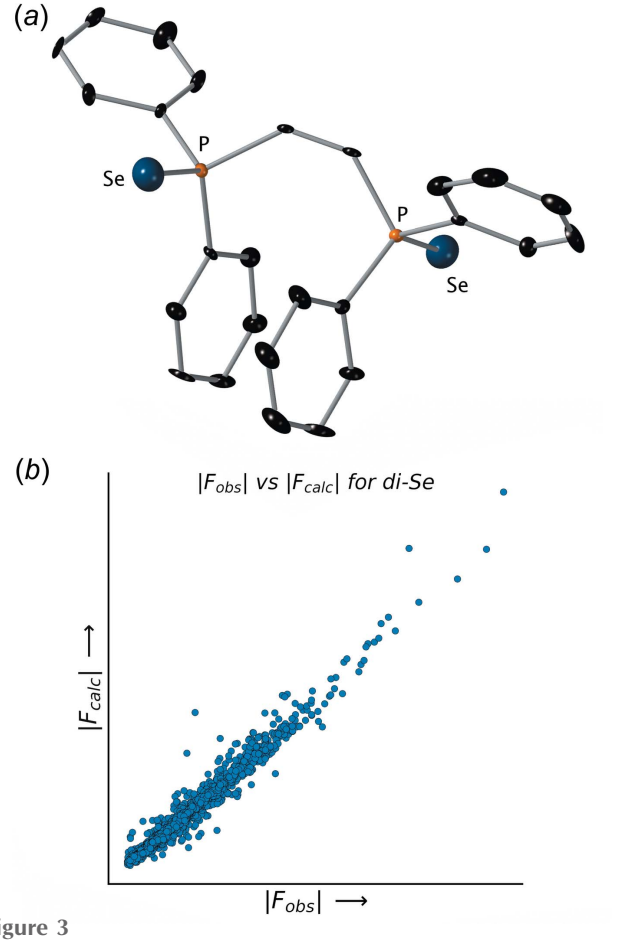

Figure 3
(*a*) An ellipsoid (50% probability) plot for the di-selenide model. Note the unrealistically large ellipsoids at the chalcogen sites and the small highly eccentric ellipsoids for the carbon atoms. (*b*) A plot of $|F_{obs}|$ *vs* $|F_{calc}|$ values for the di-selenide model. Note the extent of scatter in the plot.

2.3. Trial 3: a mono-selenide/di-selenide solid-solution model

Since atomic scattering factors are (to a first approximation) proportional to atomic number, refinement of the occupancies at the chalcogen sites should give a good estimate of the

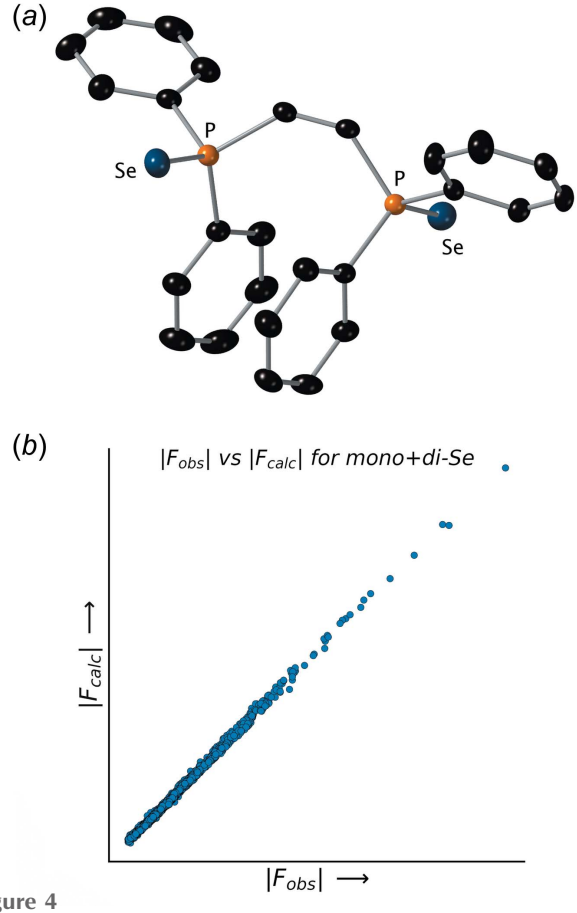

Figure 4
(*a*) An ellipsoid (50% probability) plot for the mixed mono-selenide/di-selenide model. Note that all ellipsoids appear quite normal. (*b*) A plot of $|F_{obs}|$ *vs* $|F_{calc}|$ values for the mixed mono-selenide/di-selenide model. Note the much reduced scatter in the plot relative to Figs. 2 and 3.

Table 3
List of the top four poorly fitting reflections for the model of the mixed mono/di-selenide shown in Fig. 4.

h k l	F^2_{obs}	F^2_{calc}	*error/s.u.*	$F_{calc}/F_{calc(max)}$	*d–spacing* (Å)
6 3 0	275.52	151.58	7.71	0.053	1.86
1 0 2	344.63	207.43	7.69	0.062	6.16
0 0 2	118.70	64.07	5.83	0.034	7.12
0 2 1	20.03	3.69	5.55	0.008	5.98

There are no egregious F^2_{obs} >> F^2_{calc} mis-matches for this model.

Table 4
List of the top four poorly fitting reflections for the model of the di-selenide shown in Fig. 5.

h k l	F^2_{obs}	F^2_{calc}	*error/s.u.*	$F_{calc}/F_{calc(max)}$	*d–spacing* (Å)
6 3 0	270.87	165.41	7.11	0.055	1.86
0 8 0	301.14	215.46	5.07	0.063	1.65
0 6 2	784.43	965.40	4.86	0.133	2.10
2 5 1	57.90	29.40	4.80	0.023	2.39

There are no egregious F^2_{obs} >> F^2_{calc} mis-matches for this model.

amount of available density. Thus, to better fit the available electron density, the occupancies at each Se atom were refined freely, which gave occupancies of 0.712 (2) and 0.655 (2) for the two chalcogen sites (Fig. 4*a*). The R_1 value dropped quite precipitously to 0.0236 and the displacement ellipsoids for all atoms appeared to be acceptable. For this model, the *checkCIF* report revealed no *B*-level alerts, and the discrepancy between the top four observed *vs* calculated mismatches was correspondingly *much* smaller than for any of the previous models (Table 3 and Fig. 4*b*).

2.4. Trial 4: a mixed selenide/sulfide solid-solution model

At this point, the statistics for the model were acceptable and *checkCIF* raised no red flags. Nonetheless, a critical comparison of the P═Se distances in the model shown in Fig. 4*a* to values listed in *International Tables for Crystallography* vol. C (Table 9.5.1.1; Prince, 2006) and updated information in the CSD (Groom *et al.*, 2016) available *via MOGUL* (Bruno *et al.*, 2004) revealed additional *chemical* evidence that the outwardly acceptable model was subtly flawed. The average length for P═Se bonds is listed in these resources as 2.093 Å, while that of P═S bonds is 1.954 Å. The lengths of the P═Se bonds in the model shown in Fig. 4*a* are in between these two values at 2.060 (8) and 2.0328 (8) Å. This observation is reminiscent of work by Gerard Parkin and co-workers in de-bunking the bond-stretch isomerism theory (Parkin, 1992), in which improbable 'bond lengths' were shown to result from undiagnosed chemical inhomogeneity rather than unrealistic bond-length differences.

In a similar vein, one logical explanation for the discrepancy in the present case was that the sample could have been contaminated with some di-sulfide **2**. These compounds were all synthesized several years ago, and the mixed Se/S compound had been one of the synthetic goals (*vide supra*). Modification of the model to include selenium and sulfur at both sites, where the occupancies of these atoms were refined to sum to unity, resulted in the model shown in Fig. 5*a* and 6. This model has an R_1 value of 0.0209, notably lower than the previous selenide-only model, with the relative sulfur-to-selenium occupancies for each site being 0.513 (3):0.487 (3) and 0.614 (3):0.386 (3). The bond lengths for this final model are also in reasonable agreement with literature averages, the P═Se distances being 2.082 (8) and 2.088 (11) Å, while the P═S distances are 2.021 (19) and 1.953 (16) Å, directly from refinement, *i.e.*, *without* distance restraints. Since the literature P═S distance is only ∼0.934 that of P═Se (*i.e.*, 1.954/2.093 *vide supra*), had the relative sulfur occupancy been much lower, then a restraint to tie the P═Se/S distances *via* an FVAR parameter in *SHELXL* might have been necessary. A look at the list of 'disagreeable' reflections also shows an improvement (Tables 1–4). Note in particular that *none* of the worst offenders in Table 1 or 2 show up in Table 4. Based on these features and statistics, the structure for **5** shown in Fig. 6 is demonstrably the superior model for this crystal.

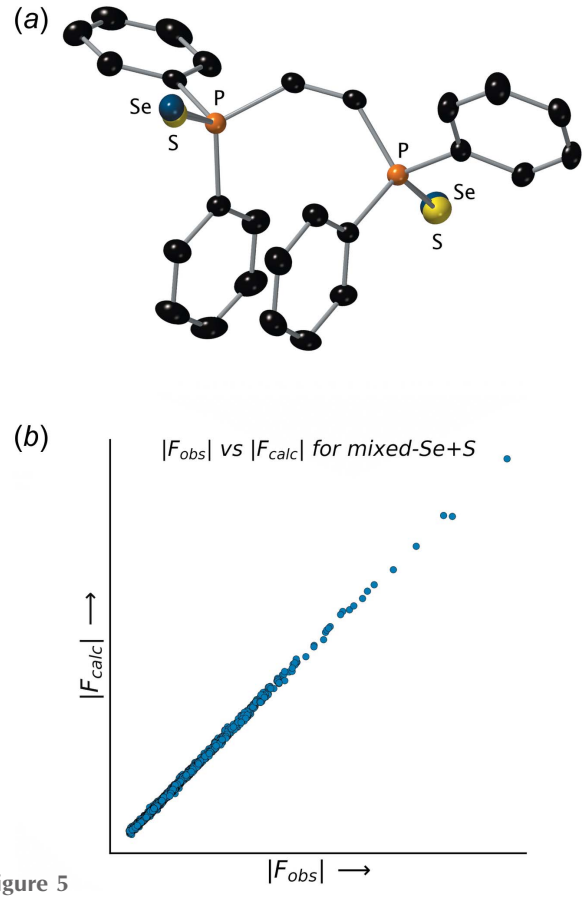

Figure 5
(*a*) An ellipsoid (50% probability) plot for the mixed selenide/sulfide model. Note that all ellipsoids appear quite normal. (*b*) A plot of $|F_{obs}|$ *vs* $|F_{calc}|$ values for the mixed selenide/sulfide model. Note the much reduced scatter in the plot relative to Figs. 2 and 3.

3. Structural commentary

The structure of **5** (Fig. 6) shares many similarities with the di-sulfide **2** (structure **I** in Rawls *et al.*, 2023) and the di-selenide **3** (Jones *et al.*, 2015). As stated in section 2.4, in spite of the superpositional disorder of Se and S at both chalcogen sites,

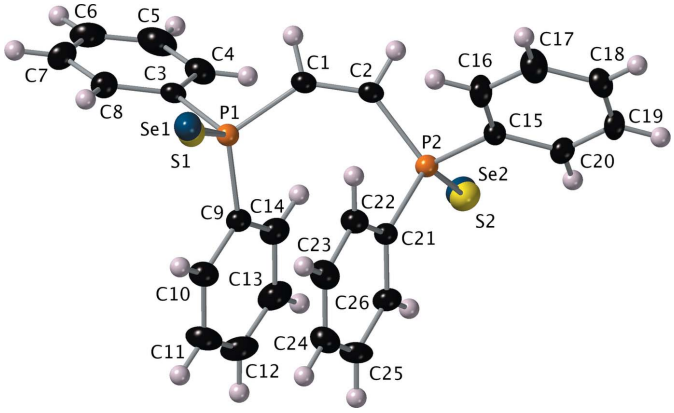

Figure 6
An ellipsoid (50% probability) plot for the final mixed selenide/sulfide model showing the atom-numbering scheme.

the unrestrained pnictogen-to-chalcogen bond distances [P1═Se1 = 2.0818 (8), P2═Se2 = 2.0879 (11), P1═S1 = 2.021 (19), P2═S2 = 1.953 (16) Å] are within or close to the normal ranges. All other bond distances and angles are also normal. There is a slight twist out of planarity at C1═C2, which gives a P1—C1—C2—P2 torsion angle of 9.0 (5)°. This, and torsion angles C9—P1—C1—C2 [−35.3 (3)°] and C1—C2—P2—C21 [−34. (3)°] effectively place phenyl rings C9–C14 and C12–C26 into an intramolecular π–π-stacking arrangement. The dihedral angle between these overlapped phenyl rings is only 5.45 (3)° although the stacking is skewed, leading to a ring centroid–centroid distance of 3.737 (4) Å.

4. Supramolecular features

The molecular packing in **5** is similar to that in the di-sulfide **2** (Rawls *et al.*, 2023) and the di-selenide **3** (Jones *et al.*, 2015). Since all hydrogen atoms are bound to carbon, there are no strong hydrogen bonds. There are also no intermolecular π–π interactions, though there are numerous weak C—H···π contacts. A Hirshfeld-surface analysis mapped over d_{norm} (Fig. 7) shows that intermolecular contacts are dominated by hydrogen, either to other hydrogen atoms (55.0% of contacts), or to carbon (24.6%), or Se/S sites (16.4%). The remainder of the contacts (C···C at 3.3% and C···Se/S at 0.7%) are negligible. The strongest interactions, however, *i.e.* those in which distances are appreciably less than the sum of van der

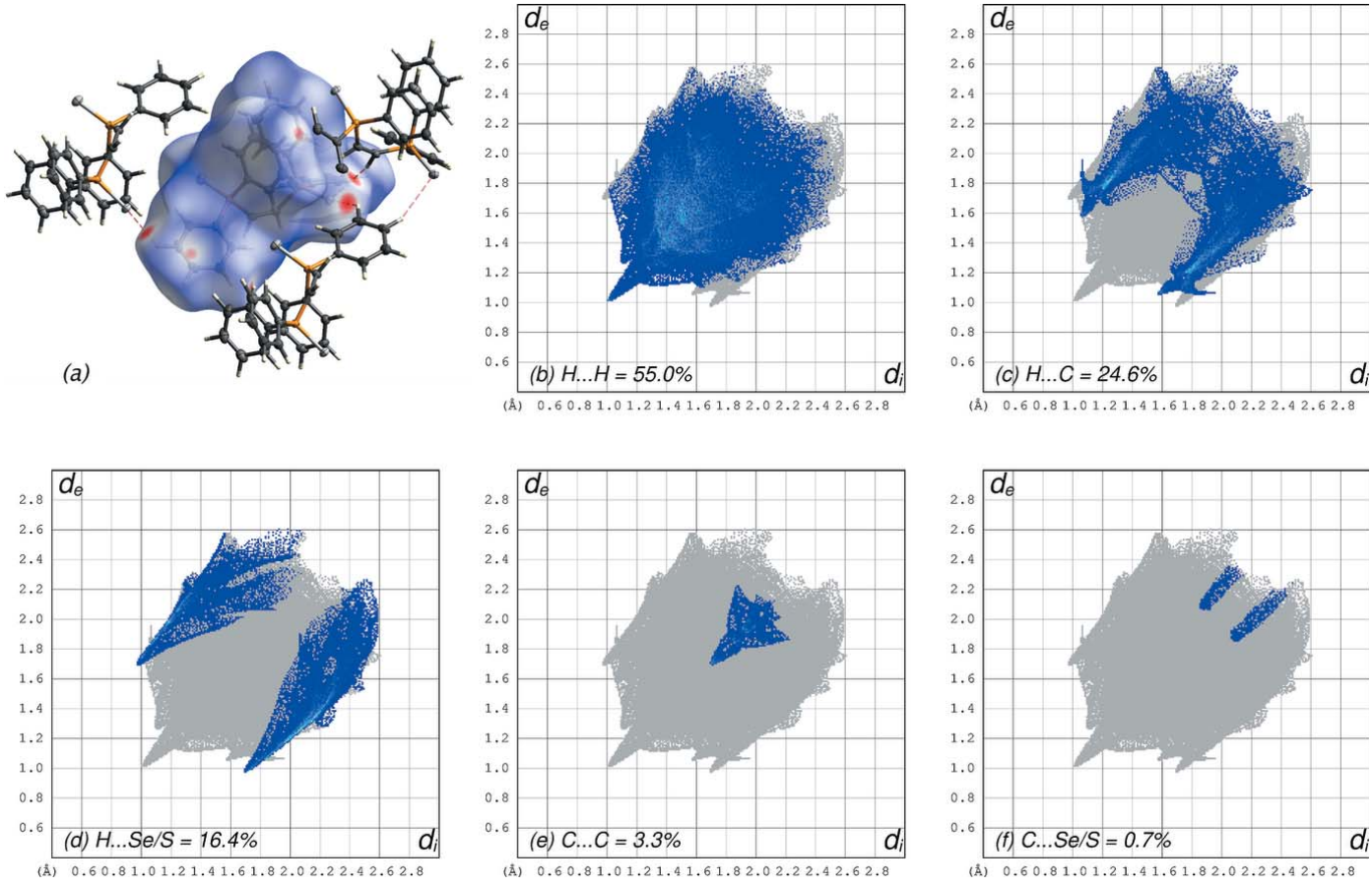

Figure 7
(*a*) A Hirshfeld-surface plot mapped over d_{norm} for the final model. Red spots and dashed lines highlight close contacts between C—H groups and the Se/S sites (see also Table 5). (*b*) Hirshfeld-surface fingerprint plot showing H···H contacts (55.0%). (*c*) Hirshfeld-surface fingerprint plot showing H···C contacts (24.6%). (*d*) Hirshfeld-surface fingerprint plot showing H···Se/S contacts (16.4%). (*e*) Hirshfeld-surface fingerprint plot showing C···C contacts (3.3%). (*f*) Hirshfeld-surface fingerprint plot showing C···Se/S contacts (0.7%).

Table 5
C—H···chalcogen close-contact geometry (Å, °).

D—H···*A*	*D*—H	H···*A*	*D*···*A*	*D*—H···*A*
C1—H1···Se2^{i}	0.95	2.87	3.752 (13)	155.1
C1—H1···S2^{i}	0.95	2.89	3.76 (2)	153.4
C8—H8···Se1	0.95	2.95	3.443 (8)	113.8
C8—H8···S1	0.95	2.82	3.325 (18)	114.5
C10—H10···Se1	0.95	2.92	3.459 (8)	117.4
C10—H10···S1	0.95	2.81	3.349 (19)	117.2
C20—H20···Se2	0.95	2.93	3.431 (13)	114.5
C20—H20···S2	0.95	2.92	3.40 (2)	112.6
C26—H26···Se2	0.95	3.00	3.524 (11)	116.6
C26—H26···S2	0.95	2.85	3.361 (17)	114.8

Symmetry code: (i) $x+\frac{1}{2}, -y+\frac{3}{2}, -z$.

Waals radii (see intense red spots in Fig. 7*a*) are from C—H···Se/S contacts (Table 5).

5. Database survey

The Cambridge Structural Database (CSD, v5.43 with all updates through Nov. 2022; Groom *et al.*, 2016) returns 5727 entries for a search fragment consisting of the dppe molecule. Of these, 895 have 'any atom' single bonded to the phosphorus and 267 are double bonded. There are 35 entries with two P═S bonds and 17 with two P═Se bonds. There are also some mixed species; 33 entries have just one P═S and two entries have just one P═Se, though these mixed structures have little else in common with structure **5** discussed herein. The closest structures to **5** are the di-selenide structures YOWTIP (Jones *et al.*, 2015) and the di-sulfide CAMCUR01 (Rawls *et al.*, 2023).

6. Refinement

A summary of data collection details and structure refinement statistics is given in Table 6. Hydrogen atoms were found in difference-Fourier maps, but subsequently included in the refinement using riding models, with constrained distances set to 0.95 Å. U_{iso}(H) values were set to $1.2U_{eq}$ of the attached carbon atom. To ensure satisfactory refinement, constraints (*SHELXL* command EADP) were used to equalize displacement parameters of superimposed Se/S atoms.

7. Conclusions

This crystal structure can serve as a straightforward instructional tool to demonstrate the varied pieces of information used to determine the quality and ultimately the correctness of a model. Here we investigated residual electron density, size of displacement ellipsoids, F_{obs}^2 and F_{calc}^2 mis-matches, plots of $|F_{obs}|$ *vs* $|F_{calc}|$ and comparison of interatomic distances to literature averages. Of particular importance is that the analysis highlights the dangers of uncritical suppression of outliers by inappropriate use of the OMIT command in *SHELXL*. Since the path to determining the best model inevitably varies from one structure to the next, a few additional points to consider, along with some background and, where appropriate, strategies to deal with them are included in the supporting information.

Table 6
Experimental details.

Crystal data	
Chemical formula	$C_{26}H_{22}P_2S_{1.13}Se_{0.87}$
M_r	501.46
Crystal system, space group	Orthorhombic, $P2_12_12_1$
Temperature (K)	173
a, *b*, *c* (Å)	12.2833 (2), 13.1643 (2), 14.2478 (2)
V (Å^3)	2303.88 (6)
Z	4
Radiation type	Cu *Kα*
μ (mm^{-1})	4.32
Crystal size (mm)	0.49 × 0.45 × 0.34
Data collection	
Diffractometer	Bruker APEXII CCD
Absorption correction	Multi-scan (*SADABS*; Krause *et al.*, 2015)
T_{min}, T_{max}	0.587, 0.754
No. of measured, independent and observed [$I > 2\sigma(I)$] reflections	24246, 4187, 4155
R_{int}	0.026
(sin $\theta/\lambda)_{max}$ (Å^{-1})	0.617
Refinement	
$R[F^2 > 2\sigma(F^2)]$, $wR(F^2)$, *S*	0.021, 0.053, 1.10
No. of reflections	4187
No. of parameters	279
H-atom treatment	H-atom parameters constrained
$\Delta\rho_{max}$, $\Delta\rho_{min}$ (e Å^{-3})	0.25, −0.23
Absolute structure	Flack *x* determined using 1619 quotients $[(I^+)-(I^-)]/[(I^+)+(I^-)]$ (Parsons *et al.*, 2013).
Absolute structure parameter	0.018 (5)

Computer programs: *APEX2* (Bruker, 2013), *SHELXT* (Sheldrick, 2015*a*), *SHELXL2019/2* (Sheldrick, 2015*b*), *OLEX2* (Dolomanov *et al.*, 2009; Bourhis *et al.*, 2015), *Mercury* (Macrae *et al.*, 2020), *ShelXle* (Hübschle *et al.*, 2011), *CrystalExplorer* (Spackman *et al.*, 2021), *CrystalMaker* (Palmer, 2007), *SHELX* (Sheldrick, 2008) and *publCIF* (Westrip, 2010).

8. Related literature

The supporting information includes a number of references that are not cited in the main paper. These sources are not exhaustive, but might serve as a useful starting point for further enquiry by an interested student. They are grouped by their respective contexts and cited here:

General advice on structure and refinement strategy: Watkin, 1994; Clegg, 2019; Linden, 2020; Spek, 2020.

Twinning: Hahn & Klapper, 2006; Donnay & Donnay, 1959; Nespolo & Ferraris, 2003; Nespolo, 2015, 2019; Nespolo *et al.*, 2020; Herbst-Irmer & Sheldrick, 1998, 2002; Parsons, 2003; Parkin, 2021; Spek, 2020; Cooper *et al.*, 2002.

Molecular geometry and crystal symmetry: Parkin, 1992; Allen *et al.*, 1987; Orpen *et al.*, 1989; Prince, 2006; Baur & Kassner, 1992; Marsh, 1997; Marsh & Spek, 2001; Le Page, 1987, 1988; Mohamed *et al.* (2016); Parkin *et al.*, 2023; Vinaya *et al.* (2023); Artioli *et al.* (1997); Parkin & Hope (1998).

Rigid-body motion and TLS analysis: Schomaker & Trueblood, 1968; Haestier *et al.*, 2008.

Absorption correction: de Meulenaer & Tompa, 1965; Blessing, 1995; Krause *et al.*, 2015.

Extinction correction: Darwin, 1914*a*,*b*; Becker & Coppens, 1974; Larson, 1967.

SQUEEZE: van der Sluis & Spek, 1990; Spek, 2015.

Spherical scattering factor approximation: Doyle & Turner, 1968; Dawson, 1964*a*,*b*; Coppens *et al.*, 1969.

Multiple diffraction: Renninger, 1937.

λ/2 effects: Kirschbaum *et al.*, 1997.

Radiation damage: Abrahams, 1973; Hope, 1975; Abrahams & Marsh, 1987; Moon *et al.*, 2011; Christensen *et al.*, 2019.

Diffuse scatter and satellite reflections: Bürgi, 2022; Stevens, 1974; Dornberger-Schiff, 1956; Zachariasen, 1967; Wagner & Schönleber, 2009; Petříček *et al.*, 2014.

Acknowledgements

We are grateful to the GVSU Chemistry Department Weldon Fund for support of this work. The CCD-based X-ray diffractometers at Michigan State University were upgraded and/or replaced using departmental funds.

Funding information

Funding for this research was provided by: NSF (RUI CHE-2102576) to SB at GVSU) and GVSU CSCE Research Grant-in-Aid to B. Rawls.

References

Abrahams, S. C. (1973). *Acta Cryst.* A**29**, 111–116.
Abrahams, S. C. & Marsh, P. (1987). *Acta Cryst.* A**43**, 265–269.
Allen, F. H., Kennard, O., Watson, D. G., Brammer, L., Orpen, A. G. & Taylor, R. (1987). *J. Chem. Soc. Perkin Trans. 2*, pp. S1–S19.
Artioli, G., Masciocchi, N. & Galli, E. (1997). *Acta Cryst.* B**53**, 498–503.
Baur, W. H. & Kassner, D. (1992). *Acta Cryst.* B**48**, 356–369.
Becker, P. J. & Coppens, P. (1974). *Acta Cryst.* A**30**, 129–147.
Blessing, R. H. (1995). *Acta Cryst.* A**51**, 33–38.
Bourhis, L. J., Dolomanov, O. V., Gildea, R. J., Howard, J. A. K. & Puschmann, H. (2015). *Acta Cryst.* A**71**, 59–75.
Bruker (2013). *APEX2*. Bruker AXS Inc., Madison, Wisconsin, USA.
Bruno, I. J., Cole, J. C., Kessler, M., Luo, J., Motherwell, W. D. S., Purkis, L. H., Smith, B. R., Taylor, R., Cooper, R. I., Harris, S. E. & Orpen, A. G. (2004). *J. Chem. Inf. Comput. Sci.* **44**, 2133–2144.
Bürgi, H.-B. (2022). *Acta Cryst.* B**78**, 283–289.
Christensen, J., Horton, P. N., Bury, C. S., Dickerson, J. L., Taberman, H., Garman, E. F. & Coles, S. J. (2019). *IUCrJ*, **6**, 703–713.
Clegg, W. (2019). *Acta Cryst.* E**75**, 1812–1819.
Cooper, R. I., Gould, R. O., Parsons, S. & Watkin, D. J. (2002). *J. Appl. Cryst.* **35**, 168–174.
Coppens, P., Sabine, T. M., Delaplane, G. & Ibers, J. A. (1969). *Acta Cryst.* B**25**, 2451–2458.
Darwin, C. G. (1914*a*). *London, Edinb. Dubl. Philos. Mag. J. Sci.* **27**, 315–333.
Darwin, C. G. (1914*b*). *London, Edinb. Dubl. Philos. Mag. J. Sci.* **27**, 675–690.
Dawson, B. (1964*a*). *Acta Cryst.* **17**, 990–996.
Dawson, B. (1964*b*). *Acta Cryst.* **17**, 997–1009.
Dolomanov, O. V., Bourhis, L. J., Gildea, R. J., Howard, J. A. K. & Puschmann, H. (2009). *J. Appl. Cryst.* **42**, 339–341.
Donnay, J. D. H. & Donnay, G. (1959). *International Tables for X-ray Crystallography*, vol. II, p104. Birmingham, Kynoch Press.
Dornberger-Schiff, K. (1956). *Acta Cryst.* **9**, 593–601.
Doyle, P. A. & Turner, P. S. (1968). *Acta Cryst.* A**24**, 390–397.
Groom, C. R., Bruno, I. J., Lightfoot, M. P. & Ward, S. C. (2016). *Acta Cryst.* B**72**, 171–179.
Haestier, J., Sadki, M., Thompson, A. L. & Watkin, D. (2008). *J. Appl. Cryst.* **41**, 531–536.
Hahn, Th. & Klapper, H. (2006). *International Tables for Crystallography*, vol. D, pp. 393–448. Chester: International Union of Crystallography.
Herbst-Irmer, R. & Sheldrick, G. M. (1998). *Acta Cryst.* B**54**, 443–449.
Herbst-Irmer, R. & Sheldrick, G. M. (2002). *Acta Cryst.* B**58**, 477–481.
Hope, H. (1975). In *Anomalous Scattering* edited by S. Ramaseshan & S. C. Abrahams, Copenhagen: IUCr, Munksgaard.
Hübschle, C. B., Sheldrick, G. M. & Dittrich, B. (2011). *J. Appl. Cryst.* **44**, 1281–1284.
Jones, P. G., Hrib, C. & du Mont, W.-W. (2015). Private Communication (refcode YOWTIP) CCDC, Cambridge, England.
Kirschbaum, K., Martin, A. & Pinkerton, A. A. (1997). *J. Appl. Cryst.* **30**, 514–516.
Krause, L., Herbst-Irmer, R., Sheldrick, G. M. & Stalke, D. (2015). *J. Appl. Cryst.* **48**, 3–10.
Larson, A. C. (1967). *Acta Cryst.* **23**, 664–665.
Le Page, Y. (1987). *J. Appl. Cryst.* **20**, 264–269.
Le Page, Y. (1988). *J. Appl. Cryst.* **21**, 983–984.
Linden, A. (2020). *Acta Cryst.* E**76**, 765–775.
Luster, T., Van de Roovaart, H. J., Korman, K. J., Sands, G. G., Dunn, K. M., Spyker, A., Staples, R. J., Biros, S. M. & Bender, J. E. (2022). *Dalton Trans.* **51**, 9103–9115.
Macrae, C. F., Sovago, I., Cottrell, S. J., Galek, P. T. A., McCabe, P., Pidcock, E., Platings, M., Shields, G. P., Stevens, J. S., Towler, M. & Wood, P. A. (2020). *J. Appl. Cryst.* **53**, 226–235.
Marsh, R. E. (1997). *Acta Cryst.* B**53**, 317–322.
Marsh, R. E. & Spek, A. L. (2001). *Acta Cryst.* B**57**, 800–805.
Meulenaer, J. de & Tompa, H. (1965). *Acta Cryst.* **19**, 1014–1018.
Mohamed, S. K., Younes, S. H. H., Abdel-Raheem, E. M. M., Horton, P. N., Akkurt, M. & Glidewell, C. (2016). *Acta Cryst.* C**72**, 57–62.
Moon, D. K., Tripathi, A., Sullivan, D., Siegler, M. A., Parkin, S. & Posner, G. H. (2011). *Bioorg. Med. Chem. Lett.* **21**, 2773–2775.
Morse, P. T., Staples, R. J. & Biros, S. M. (2016). *Polyhedron*, **114**, 2–12.
Mugemana, J., Bender, J., Staples, R. J. & Biros, S. M. (2018). *Acta Cryst.* E**74**, 998–1001.
Neils, T., LaDuca, A., Bender, J. E., Staples, R. J. & Biros, S. M. (2022). *Acta Cryst.* E**78**, 1044–1047.
Nespolo, M. (2015). *Cryst. Res. Technol.* **50**, 362–371.
Nespolo, M. (2019). *Acta Cryst.* A**75**, 551–573.
Nespolo, M. & Ferraris, G. (2003). *Z. Kristallogr.* **218**, 178–181.
Nespolo, M., Smaha, R. W. & Parkin, S. (2020). *Acta Cryst.* B**76**, 643–649.
Orpen, A. G., Brammer, L., Allen, F. H., Kennard, O., Watson, D. G. & Taylor, R. (1989). *J. Chem. Soc. Dalton Trans.* pp. S1.
Palmer, D. (2007). *CrystalMaker*. CrystalMaker Software Ltd, Yarnton, England.
Parkin, G. (1992). *Acc. Chem. Res.* **25**, 455–460.
Parkin, S., Glidewell, C. & Horton, P. N. (2023). *Acta Cryst.* C**79**, 77–82.
Parkin, S. & Hope, H. (1998). *Acta Cryst.* B**54**, 339–344.
Parkin, S. R. (2021). *Acta Cryst.* E**77**, 452–465.
Parsons, S. (2003). *Acta Cryst.* D**59**, 1995–2003.
Parsons, S., Flack, H. D. & Wagner, T. (2013). *Acta Cryst.* B**69**, 249–259.
Petříček, V., Dušek, M. & Plášil, J. (2014). *Z. Kristallogr.* **229**, 345–352.
Prince, E. (2006). *International Tables for Crystallography*, vol. C. Table 9.5.1.1. Chester: International Union of Crystallography.
Rawls, B., Cunningham, J., Bender, J. E., Staples, R. J. & Biros, S. M. (2023). *Acta Cryst.* E**79**, 28–32.
Renninger, M. (1937). *Z. Phys.* **106**, 141–176.
Schomaker, V. & Trueblood, K. N. (1968). *Acta Cryst.* B**24**, 63–76.

Sheldrick, G. M. (2008). *Acta Cryst.* A**64**, 112–122.
Sheldrick, G. M. (2015*a*). *Acta Cryst.* A**71**, 3–8.
Sheldrick, G. M. (2015*b*). *Acta Cryst.* C**71**, 3–8.
Sluis, P. van der & Spek, A. L. (1990). *Acta Cryst.* A**46**, 194–201.
Spackman, P. R., Turner, M. J., McKinnon, J. J., Wolff, S. K., Grimwood, D. J., Jayatilaka, D. & Spackman, M. A. (2021). *J. Appl. Cryst.* **54**, 1006–1011.
Spek, A. L. (2015). *Acta Cryst.* C**71**, 9–18.
Spek, A. L. (2020). *Acta Cryst.* E**76**, 1–11.
Stevens, E. D. (1974). *Acta Cryst.* A**30**, 184–189.
Vinaya, Basavaraju, Y. B., Srinivasa, G. R., Shreenivas, M. T., Yathirajan, H. S. & Parkin, S. (2023). *Acta Cryst.* E**79**, 54–59.
Wagner, T. & Schönleber, A. (2009). *Acta Cryst.* B**65**, 249–268.
Watkin, D. (1994). *Acta Cryst.* A**50**, 411–437.
Westrip, S. P. (2010). *J. Appl. Cryst.* **43**, 920–925.
Zachariasen, W. H. (1967). *Acta Cryst.* **23**, 44–49.

supporting information

Acta Cryst. (2023). E**79**, 246-253 [https://doi.org/10.1107/S2056989023002700]

A mixed phosphine sulfide/selenide structure as an instructional example for how to evaluate the quality of a model

Sean Parkin, Jeremy Cunningham, Brian Rawls, John E. Bender, Richard J. Staples and Shannon M. Biros

Computing details

Data collection: *APEX2* (Bruker, 2013); cell refinement: *APEX2* (Bruker, 2013); data reduction: *APEX2* (Bruker, 2013); program(s) used to solve structure: *SHELXT* (Sheldrick, 2015a); program(s) used to refine structure: *SHELXL2019/2* (Sheldrick, 2015b); molecular graphics: *Olex2* (Dolomanov *et al.*, 2009; Bourhis *et al.*, 2015), *Mercury* (Macrae *et al.*, 2020), *ShelXle* (Hübschle *et al.*, 2011), *CrystalExplorer* (Spackman *et al.*, 2021), *CrystalMaker* (Palmer, 2007); software used to prepare material for publication: *SHELX* (Sheldrick, 2008) and *publCIF* (Westrip, 2010).

1,2-(Ethene-1,2-diyl)bis(diphenylphoshpine sulfide/selenide)

Crystal data

$C_{26}H_{22}P_2S_{1.13}Se_{0.87}$
M_r = 501.46
Orthorhombic, $P2_12_12_1$
a = 12.2833 (2) Å
b = 13.1643 (2) Å
c = 14.2478 (2) Å
V = 2303.88 (6) Å^3
Z = 4
$F(000)$ = 1023
D_x = 1.446 Mg m^{-3}
Cu $K\alpha$ radiation, λ = 1.54178 Å
Cell parameters from 9858 reflections
θ = 3.1–72.1°
μ = 4.32 mm^{-1}
T = 173 K
Block, yellow
0.49 × 0.45 × 0.34 mm

Data collection

Bruker APEXII CCD diffractometer
Radiation source: microsource
Detector resolution: 7.41 pixels mm^{-1}
φ and ω scans
Absorption correction: multi-scan (*SADABS*; Krause *et al.*, 2015)
T_{min} = 0.587, T_{max} = 0.754
24246 measured reflections
4187 independent reflections
4155 reflections with $I > 2\sigma(I)$
R_{int} = 0.026
θ_{max} = 72.0°, θ_{min} = 4.6°
h = −13→14
k = −15→16
l = −17→17

Refinement

Refinement on F^2
Least-squares matrix: full
$R[F^2 > 2\sigma(F^2)]$ = 0.021
$wR(F^2)$ = 0.053
S = 1.10
4187 reflections
279 parameters
0 restraints
Primary atom site location: structure-invariant direct methods
Secondary atom site location: difference Fourier map
Hydrogen site location: difference Fourier map
H-atom parameters constrained

$w = 1/[\sigma^2(F_o^2) + (0.0259P)^2 + 0.6437P]$
where $P = (F_o^2 + 2F_c^2)/3$
$(\Delta/\sigma)_{max} < 0.001$
$\Delta\rho_{max} = 0.25$ e Å^{-3}
$\Delta\rho_{min} = -0.23$ e Å^{-3}

Absolute structure: Flack *x* determined using 1619 quotients $[(I^+)-(I^-)]/[(I^+)+(I^-)]$ (Parsons *et al.*, 2013).
Absolute structure parameter: 0.018 (5)

Special details

Geometry. All esds (except the esd in the dihedral angle between two l.s. planes) are estimated using the full covariance matrix. The cell esds are taken into account individually in the estimation of esds in distances, angles and torsion angles; correlations between esds in cell parameters are only used when they are defined by crystal symmetry. An approximate (isotropic) treatment of cell esds is used for estimating esds involving l.s. planes.

Refinement. Refinement progress was checked using *Platon* (Spek, 2020) and by an *R*-tensor (Parkin, 2000). The final model was further checked with the IUCr utility *checkCIF*.

Fractional atomic coordinates and isotropic or equivalent isotropic displacement parameters (Å^2)

	x	*y*	*z*	U_{iso}*/U_{eq}	Occ. (<1)
Se1	0.5609 (7)	0.3728 (6)	0.1269 (5)	0.0324 (6)	0.487 (3)
S1	0.5543 (16)	0.3748 (14)	0.1378 (11)	0.0324 (6)	0.513 (3)
Se2	0.3955 (11)	0.8180 (7)	−0.0416 (9)	0.0290 (8)	0.386 (3)
S2	0.3917 (16)	0.8053 (11)	−0.0401 (14)	0.0290 (8)	0.614 (3)
P1	0.53848 (5)	0.52619 (4)	0.15679 (4)	0.02193 (15)	
P2	0.44544 (5)	0.67007 (4)	−0.07209 (4)	0.02106 (15)	
C1	0.6036 (2)	0.60331 (18)	0.06839 (17)	0.0247 (5)	
H1	0.678166	0.615265	0.082046	0.030*	
C2	0.5726 (2)	0.64761 (18)	−0.01138 (17)	0.0238 (5)	
H2	0.632873	0.674300	−0.045092	0.029*	
C3	0.6118 (2)	0.56693 (18)	0.26141 (17)	0.0236 (5)	
C4	0.6416 (2)	0.6674 (2)	0.2747 (2)	0.0348 (6)	
H4	0.622485	0.717086	0.229226	0.042*	
C5	0.6993 (3)	0.6958 (2)	0.3544 (2)	0.0400 (7)	
H5	0.719472	0.764842	0.363164	0.048*	
C6	0.7273 (2)	0.6241 (2)	0.42085 (19)	0.0340 (6)	
H6	0.767453	0.643337	0.475021	0.041*	
C7	0.6967 (2)	0.5248 (2)	0.4079 (2)	0.0368 (7)	
H7	0.715302	0.475575	0.453854	0.044*	
C8	0.6394 (2)	0.4953 (2)	0.3293 (2)	0.0317 (6)	
H8	0.618731	0.426310	0.321502	0.038*	
C9	0.3993 (2)	0.56668 (18)	0.17259 (17)	0.0218 (5)	
C10	0.3177 (2)	0.4942 (2)	0.17614 (18)	0.0283 (6)	
H10	0.335274	0.424196	0.170070	0.034*	
C11	0.2103 (2)	0.5237 (2)	0.1886 (2)	0.0351 (6)	
H11	0.154201	0.474094	0.190052	0.042*	
C12	0.1851 (2)	0.6251 (2)	0.1987 (2)	0.0352 (6)	
H12	0.111475	0.645133	0.207103	0.042*	
C13	0.2660 (2)	0.6977 (2)	0.1968 (2)	0.0328 (6)	
H13	0.248108	0.767397	0.204846	0.039*	
C14	0.3735 (2)	0.6691 (2)	0.18307 (18)	0.0284 (6)	
H14	0.429257	0.719055	0.180830	0.034*	

C15	0.4883 (2)	0.65684 (19)	−0.19416 (17)	0.0249 (5)
C16	0.5588 (2)	0.5791 (2)	−0.22096 (19)	0.0330 (6)
H16	0.587585	0.533907	−0.175276	0.040*
C17	0.5868 (2)	0.5682 (3)	−0.3148 (2)	0.0455 (8)
H17	0.635568	0.515905	−0.333409	0.055*
C18	0.5438 (3)	0.6331 (3)	−0.3812 (2)	0.0478 (8)
H18	0.561813	0.624394	−0.445494	0.057*
C19	0.4755 (3)	0.7097 (3)	−0.3548 (2)	0.0427 (8)
H19	0.447116	0.754619	−0.400929	0.051*
C20	0.4470 (2)	0.7225 (2)	−0.26115 (19)	0.0322 (6)
H20	0.399383	0.775975	−0.243210	0.039*
C21	0.3461 (2)	0.56962 (18)	−0.05739 (17)	0.0241 (5)
C22	0.3769 (2)	0.46794 (19)	−0.06166 (18)	0.0308 (6)
H22	0.451777	0.450049	−0.064155	0.037*
C23	0.2976 (3)	0.3930 (2)	−0.0622 (2)	0.0379 (7)
H23	0.318227	0.323468	−0.064779	0.045*
C24	0.1892 (3)	0.4188 (2)	−0.0591 (2)	0.0431 (8)
H24	0.135332	0.367069	−0.060500	0.052*
C25	0.1579 (2)	0.5197 (3)	−0.0541 (2)	0.0434 (7)
H25	0.082874	0.536992	−0.051575	0.052*
C26	0.2364 (2)	0.5956 (2)	−0.05262 (19)	0.0308 (6)
H26	0.215389	0.664886	−0.048398	0.037*

Atomic displacement parameters (Å²)

	U^{11}	U^{22}	U^{33}	U^{12}	U^{13}	U^{23}
Se1	0.0372 (10)	0.0261 (4)	0.0338 (16)	0.0063 (5)	0.0091 (10)	−0.0022 (9)
S1	0.0372 (10)	0.0261 (4)	0.0338 (16)	0.0063 (5)	0.0091 (10)	−0.0022 (9)
Se2	0.0335 (8)	0.017 (2)	0.0367 (4)	0.0043 (14)	−0.0011 (5)	−0.0014 (14)
S2	0.0335 (8)	0.017 (2)	0.0367 (4)	0.0043 (14)	−0.0011 (5)	−0.0014 (14)
P1	0.0201 (3)	0.0209 (3)	0.0248 (3)	0.0025 (2)	0.0022 (2)	0.0025 (2)
P2	0.0204 (3)	0.0208 (3)	0.0220 (3)	0.0002 (3)	0.0002 (2)	0.0000 (2)
C1	0.0179 (11)	0.0297 (13)	0.0266 (12)	−0.0028 (10)	0.0015 (10)	0.0006 (10)
C2	0.0188 (12)	0.0270 (12)	0.0257 (12)	−0.0018 (9)	0.0015 (9)	−0.0016 (9)
C3	0.0199 (12)	0.0272 (12)	0.0238 (12)	0.0052 (10)	0.002 (1)	0.0034 (10)
C4	0.0413 (16)	0.0288 (13)	0.0342 (14)	0.0031 (12)	−0.0110 (12)	0.0067 (11)
C5	0.0461 (17)	0.0342 (15)	0.0397 (16)	0.0021 (13)	−0.0112 (14)	0.0000 (13)
C6	0.0269 (13)	0.0500 (16)	0.0253 (13)	0.0059 (13)	−0.0039 (11)	0.0015 (12)
C7	0.0303 (14)	0.0482 (17)	0.0318 (14)	0.0078 (13)	−0.0021 (12)	0.0178 (13)
C8	0.0287 (14)	0.0316 (13)	0.0350 (14)	0.0038 (11)	0.0024 (12)	0.0119 (11)
C9	0.0195 (11)	0.0240 (11)	0.0219 (11)	0.0003 (10)	0.0022 (10)	0.0004 (9)
C10	0.0276 (13)	0.0263 (13)	0.0312 (13)	−0.0050 (11)	0.0045 (11)	−0.0004 (11)
C11	0.0237 (13)	0.0425 (16)	0.0393 (16)	−0.0091 (12)	0.0070 (12)	−0.0019 (13)
C12	0.0206 (13)	0.0506 (16)	0.0345 (14)	0.0065 (13)	0.0053 (11)	−0.0017 (13)
C13	0.0298 (15)	0.0299 (14)	0.0387 (15)	0.0083 (12)	0.0024 (12)	−0.0046 (11)
C14	0.0256 (13)	0.0267 (12)	0.0329 (13)	−0.0022 (11)	0.0002 (11)	−0.0014 (11)
C15	0.0196 (12)	0.0323 (14)	0.0227 (12)	−0.0076 (10)	−0.0006 (9)	−0.0024 (10)
C16	0.0255 (13)	0.0417 (14)	0.0318 (13)	−0.0013 (13)	−0.0001 (12)	−0.0085 (12)

C17	0.0290 (16)	0.064 (2)	0.0436 (18)	−0.0032 (15)	0.0073 (13)	−0.0202 (15)
C18	0.0373 (17)	0.080 (2)	0.0257 (14)	−0.0235 (18)	0.0070 (13)	−0.0069 (15)
C19	0.0452 (18)	0.0580 (19)	0.0250 (13)	−0.0177 (15)	−0.0022 (13)	0.0084 (13)
C20	0.0331 (14)	0.0324 (13)	0.0310 (13)	−0.0065 (12)	−0.0036 (13)	0.0025 (11)
C21	0.0245 (12)	0.0256 (12)	0.0223 (12)	−0.0031 (10)	0.0015 (10)	−0.001 (1)
C22	0.0333 (15)	0.0271 (13)	0.0321 (14)	0.0001 (11)	0.0062 (12)	−0.0013 (11)
C23	0.0496 (18)	0.0292 (14)	0.0348 (15)	−0.0089 (13)	0.0087 (13)	−0.0036 (12)
C24	0.0457 (18)	0.0461 (17)	0.0375 (16)	−0.0249 (15)	0.0081 (14)	−0.0064 (14)
C25	0.0254 (14)	0.0600 (19)	0.0448 (17)	−0.0114 (14)	0.0044 (13)	−0.0066 (15)
C26	0.0255 (13)	0.0344 (14)	0.0327 (14)	−0.0004 (11)	0.0045 (11)	−0.0032 (11)

Geometric parameters (Å, º)

Se1—P1	2.082 (8)	C11—H11	0.9500
S1—P1	2.021 (19)	C12—C13	1.379 (4)
Se2—P2	2.088 (11)	C12—H12	0.9500
S2—P2	1.953 (16)	C13—C14	1.387 (4)
P1—C1	1.805 (2)	C13—H13	0.9500
P1—C9	1.805 (2)	C14—H14	0.9500
P1—C3	1.822 (3)	C15—C20	1.384 (4)
P2—C2	1.810 (2)	C15—C16	1.394 (4)
P2—C21	1.812 (2)	C16—C17	1.388 (4)
P2—C15	1.826 (2)	C16—H16	0.9500
C1—C2	1.333 (3)	C17—C18	1.379 (5)
C1—H1	0.9500	C17—H17	0.9500
C2—H2	0.9500	C18—C19	1.364 (5)
C3—C4	1.386 (4)	C18—H18	0.9500
C3—C8	1.392 (4)	C19—C20	1.390 (4)
C4—C5	1.389 (4)	C19—H19	0.9500
C4—H4	0.9500	C20—H20	0.9500
C5—C6	1.381 (4)	C21—C26	1.391 (4)
C5—H5	0.9500	C21—C22	1.392 (4)
C6—C7	1.373 (4)	C22—C23	1.387 (4)
C6—H6	0.9500	C22—H22	0.9500
C7—C8	1.378 (4)	C23—C24	1.375 (5)
C7—H7	0.9500	C23—H23	0.9500
C8—H8	0.9500	C24—C25	1.384 (5)
C9—C10	1.385 (4)	C24—H24	0.9500
C9—C14	1.393 (3)	C25—C26	1.389 (4)
C10—C11	1.386 (4)	C25—H25	0.9500
C10—H10	0.9500	C26—H26	0.9500
C11—C12	1.378 (4)		
C1—P1—C9	109.91 (11)	C12—C11—C10	119.9 (3)
C1—P1—C3	100.74 (12)	C12—C11—H11	120.0
C9—P1—C3	106.22 (11)	C10—C11—H11	120.0
C1—P1—S1	114.8 (5)	C11—C12—C13	120.5 (3)
C9—P1—S1	113.5 (6)	C11—C12—H12	119.7

C3—P1—S1	110.6 (6)	C13—C12—H12	119.7
C1—P1—Se1	110.1 (2)	C12—C13—C14	120.0 (3)
C9—P1—Se1	115.9 (2)	C12—C13—H13	120.0
C3—P1—Se1	112.8 (2)	C14—C13—H13	120.0
C2—P2—C21	114.01 (12)	C13—C14—C9	119.7 (2)
C2—P2—C15	100.99 (11)	C13—C14—H14	120.2
C21—P2—C15	103.59 (11)	C9—C14—H14	120.2
C2—P2—S2	109.2 (6)	C20—C15—C16	119.8 (2)
C21—P2—S2	114.3 (6)	C20—C15—P2	119.4 (2)
C15—P2—S2	114.0 (6)	C16—C15—P2	120.7 (2)
C2—P2—Se2	107.8 (4)	C17—C16—C15	119.6 (3)
C21—P2—Se2	117.3 (4)	C17—C16—H16	120.2
C15—P2—Se2	111.9 (4)	C15—C16—H16	120.2
C2—C1—P1	135.6 (2)	C18—C17—C16	120.1 (3)
C2—C1—H1	112.2	C18—C17—H17	120.0
P1—C1—H1	112.2	C16—C17—H17	120.0
C1—C2—P2	136.5 (2)	C19—C18—C17	120.3 (3)
C1—C2—H2	111.7	C19—C18—H18	119.8
P2—C2—H2	111.7	C17—C18—H18	119.8
C4—C3—C8	119.1 (2)	C18—C19—C20	120.6 (3)
C4—C3—P1	121.56 (19)	C18—C19—H19	119.7
C8—C3—P1	119.3 (2)	C20—C19—H19	119.7
C3—C4—C5	120.2 (3)	C15—C20—C19	119.6 (3)
C3—C4—H4	119.9	C15—C20—H20	120.2
C5—C4—H4	119.9	C19—C20—H20	120.2
C6—C5—C4	120.2 (3)	C26—C21—C22	120.1 (2)
C6—C5—H5	119.9	C26—C21—P2	118.59 (19)
C4—C5—H5	119.9	C22—C21—P2	120.9 (2)
C7—C6—C5	119.3 (3)	C23—C22—C21	119.6 (3)
C7—C6—H6	120.3	C23—C22—H22	120.2
C5—C6—H6	120.3	C21—C22—H22	120.2
C6—C7—C8	121.2 (3)	C24—C23—C22	120.2 (3)
C6—C7—H7	119.4	C24—C23—H23	119.9
C8—C7—H7	119.4	C22—C23—H23	119.9
C7—C8—C3	119.8 (3)	C23—C24—C25	120.5 (3)
C7—C8—H8	120.1	C23—C24—H24	119.7
C3—C8—H8	120.1	C25—C24—H24	119.7
C10—C9—C14	119.9 (2)	C24—C25—C26	119.9 (3)
C10—C9—P1	119.12 (19)	C24—C25—H25	120.1
C14—C9—P1	120.98 (19)	C26—C25—H25	120.1
C9—C10—C11	120.0 (2)	C25—C26—C21	119.7 (3)
C9—C10—H10	120.0	C25—C26—H26	120.2
C11—C10—H10	120.0	C21—C26—H26	120.2

C9—P1—C1—C2	−35.3 (3)	C11—C12—C13—C14	1.0 (4)
C3—P1—C1—C2	−147.1 (3)	C12—C13—C14—C9	−0.9 (4)
S1—P1—C1—C2	94.1 (7)	C10—C9—C14—C13	−0.2 (4)
Se1—P1—C1—C2	93.6 (4)	P1—C9—C14—C13	−178.8 (2)

P1—C1—C2—P2	9.0 (5)	C2—P2—C15—C20	−140.0 (2)
C21—P2—C2—C1	−34.1 (3)	C21—P2—C15—C20	101.8 (2)
C15—P2—C2—C1	−144.5 (3)	S2—P2—C15—C20	−23.0 (7)
S2—P2—C2—C1	95.1 (6)	Se2—P2—C15—C20	−25.5 (4)
Se2—P2—C2—C1	98.1 (5)	C2—P2—C15—C16	42.5 (2)
C1—P1—C3—C4	38.4 (3)	C21—P2—C15—C16	−75.8 (2)
C9—P1—C3—C4	−76.2 (2)	S2—P2—C15—C16	159.5 (6)
S1—P1—C3—C4	160.2 (6)	Se2—P2—C15—C16	156.9 (4)
Se1—P1—C3—C4	155.8 (3)	C20—C15—C16—C17	−0.1 (4)
C1—P1—C3—C8	−141.1 (2)	P2—C15—C16—C17	177.4 (2)
C9—P1—C3—C8	104.3 (2)	C15—C16—C17—C18	−0.9 (4)
S1—P1—C3—C8	−19.3 (6)	C16—C17—C18—C19	1.4 (5)
Se1—P1—C3—C8	−23.7 (3)	C17—C18—C19—C20	−0.9 (5)
C8—C3—C4—C5	0.7 (4)	C16—C15—C20—C19	0.6 (4)
P1—C3—C4—C5	−178.8 (2)	P2—C15—C20—C19	−177.0 (2)
C3—C4—C5—C6	0.0 (5)	C18—C19—C20—C15	0.0 (4)
C4—C5—C6—C7	−0.7 (5)	C2—P2—C21—C26	145.1 (2)
C5—C6—C7—C8	0.6 (4)	C15—P2—C21—C26	−106.1 (2)
C6—C7—C8—C3	0.1 (4)	S2—P2—C21—C26	18.5 (7)
C4—C3—C8—C7	−0.8 (4)	Se2—P2—C21—C26	17.7 (5)
P1—C3—C8—C7	178.8 (2)	C2—P2—C21—C22	−42.3 (2)
C1—P1—C9—C10	133.8 (2)	C15—P2—C21—C22	66.5 (2)
C3—P1—C9—C10	−118.1 (2)	S2—P2—C21—C22	−168.9 (7)
S1—P1—C9—C10	3.7 (6)	Se2—P2—C21—C22	−169.7 (4)
Se1—P1—C9—C10	8.1 (3)	C26—C21—C22—C23	0.8 (4)
C1—P1—C9—C14	−47.5 (2)	P2—C21—C22—C23	−171.8 (2)
C3—P1—C9—C14	60.6 (2)	C21—C22—C23—C24	0.4 (4)
S1—P1—C9—C14	−177.6 (5)	C22—C23—C24—C25	−0.9 (5)
Se1—P1—C9—C14	−173.2 (3)	C23—C24—C25—C26	0.4 (5)
C14—C9—C10—C11	1.1 (4)	C24—C25—C26—C21	0.7 (4)
P1—C9—C10—C11	179.8 (2)	C22—C21—C26—C25	−1.3 (4)
C9—C10—C11—C12	−0.9 (4)	P2—C21—C26—C25	171.4 (2)
C10—C11—C12—C13	−0.1 (4)		

Hydrogen-bond geometry (Å, º)

D—H···*A*	*D*—H	H···*A*	*D*···*A*	*D*—H···*A*
C1—H1···Se2^{i}	0.95	2.87	3.752 (13)	155
C1—H1···S2^{i}	0.95	2.89	3.76 (2)	153
C8—H8···Se1	0.95	2.95	3.443 (8)	114
C8—H8···S1	0.95	2.82	3.325 (18)	115
C10—H10···Se1	0.95	2.92	3.459 (8)	117
C10—H10···S1	0.95	2.81	3.349 (19)	117
C20—H20···Se2	0.95	2.93	3.431 (13)	115
C20—H20···S2	0.95	2.92	3.40 (2)	113

C26—H26···Se2	0.95	3.00	3.524 (11)	117
C26—H26···S2	0.95	2.85	3.361 (17)	115

Symmetry code: (i) $x+1/2, -y+3/2, -z$.